FIGURE 1

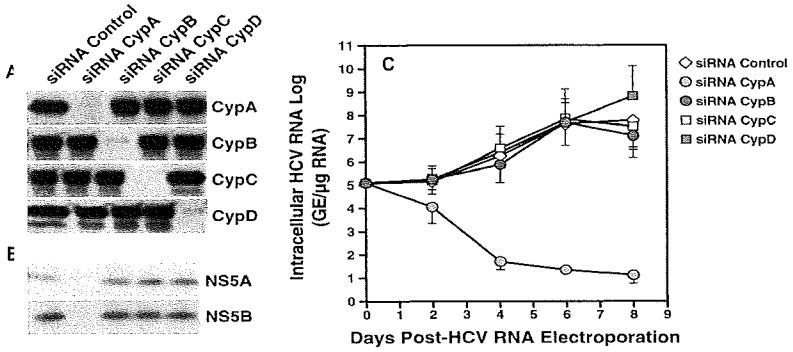

FIGURE 2

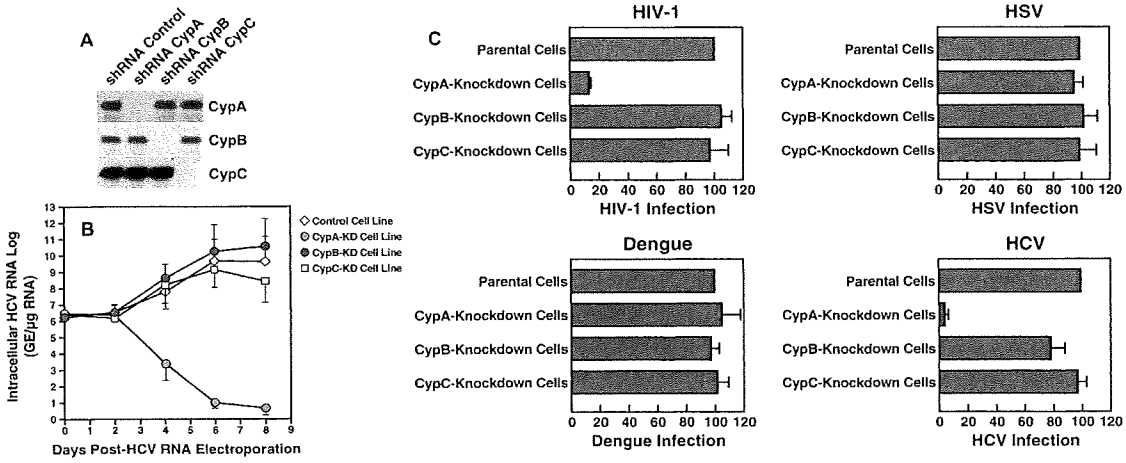

FIGURE 3

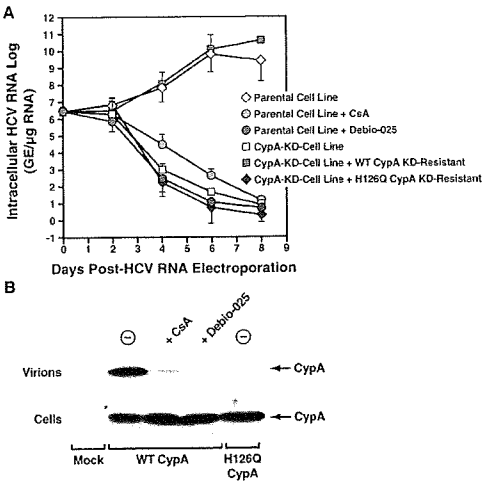

FIGURE 4

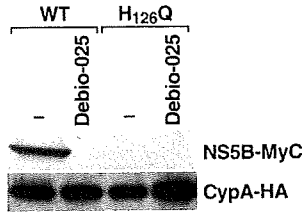

Adoptive immunotherapy with liver allograft–derived lymphocytes induces anti-HCV activity after liver transplantation in humans and humanized mice

Masahiro Ohira,[1,2] Kohei Ishiyama,[1,2] Yuka Tanaka,[1,2] Marlen Doskali,[1,2] Yuka Igarashi,[1,2] Hirotaka Tashiro,[1,2] Nobuhiko Hiraga,[2,3] Michio Imamura,[2,3] Naoya Sakamoto,[4] Toshimasa Asahara,[1,2] Kazuaki Chayama,[2,3] and Hideki Ohdan[1,2]

[1]Department of Surgery, Division of Frontier Medical Science, Programs for Biomedical Research, Graduate School of Biomedical Sciences, [2]Liver Research Project Center, and [3]Department of Medicine and Molecular Science, Division of Frontier Medical Science, Programs for Biomedical Research, Graduate School of Biomedical Sciences, Hiroshima University, Minami-ku, Hiroshima, Japan. [4]Department of Gastroenterology and Hepatology, Tokyo Medical and Dental University, Bunkyo-ku, Tokyo, Japan.

After liver transplantation in HCV-infected patients, the virus load inevitably exceeds pre-transplantation levels. This phenomenon reflects suppression of the host-effector immune responses that control HCV replication by the immunosuppressive drugs used to prevent rejection of the transplanted liver. Here, we describe an adoptive immunotherapy approach, using lymphocytes extracted from liver allograft perfusate (termed herein liver allograft–derived lymphocytes), which includes an abundance of NK/NKT cells that mounted an anti-HCV response in HCV-infected liver transplantation recipients, despite the immunosuppressive environment. This therapy involved intravenously injecting patients 3 days after liver transplantation with liver allograft–derived lymphocytes treated with IL-2 and the CD3-specific mAb OKT3. During the first month after liver transplantation, the HCV RNA titers in the sera of recipients who received immunotherapy were markedly lower than those in the sera of recipients who did not receive immunotherapy. We further explored these observations in human hepatocyte–chimeric mice, in which mouse hepatocytes were replaced by human hepatocytes. These mice unfailingly developed HCV infections after inoculation with HCV-infected human serum. However, injection of human liver–derived lymphocytes treated with IL-2/OKT3 completely prevented HCV infection. Furthermore, an in vitro study using genomic HCV replicon–containing hepatic cells revealed that IFN-γ–secreting cells played a pivotal role in such anti-HCV responses. Thus, our study presents what we believe to be a novel paradigm for the inhibition of HCV replication in HCV-infected liver transplantation recipients.

Introduction

Liver failure and hepatocellular carcinoma (HCC) due to chronic hepatitis C infection are the most common indications for liver transplantation (LT), and the incidences of both have been projected to increase further in the future. Recurrent HCV infection of the allograft is universal, occurs immediately after LT, and is associated with accelerated progression to cirrhosis, graft loss, and death (1, 2). This reflects the suppression of those host-effector immune responses that usually control HCV replication, suggesting that the immunosuppressive environment may play a major role in the rapid progression of recurrent HCV infection after LT (3, 4). Further, the immunosuppressive condition described above is considered to increase the incidence of cancer recurrence after LT in HCC patients. We recently proposed the novel strategy of adjuvant immunotherapy for preventing the recurrence of HCC after LT; this immunotherapy involves intravenously injecting LT recipients with activated liver allograft–derived NK cells (5, 6). Since the immunosuppressive regimen currently used after LT reduces the adaptive immune components but effectively maintains the innate components of cellular immunity (7–9), the augmentation of the NK cell response, which is thought to play a pivotal role in innate immunity, may be a promising immunotherapeutic approach (6). We confirmed that the IL-2/anti-CD3 mAb–treated (IL-2/OKT3–treated) liver allograft–derived NK cells expressed a significantly high level of the tumor necrosis factor–related apoptosis-inducing ligand (TRAIL), which is a critical molecule for tumor cell killing. Further, these cells showed high cytotoxicity against HCC cells, with no such effect on normal cells (5). After obtaining approval from the ethical committee of our institute, we successfully administered adoptive immunotherapy with IL-2/OKT3–treated liver lymphocytes to liver cirrhosis patients with HCC in a phase I trial. Although the long-term benefits of this approach with regard to the control of HCC recurrence after LT remain to be elucidated, this trial provided a unique opportunity to study whether the adoptive administration of IL-2/OKT3–treated liver lymphocytes could also mount an anti-HCV response in HCV-infected LT recipients.

Previous studies have highlighted the important roles of innate lymphocytes in developing immunity against hepatotropic viruses, including HCV (10, 11). In this regard, it is known that patients with chronic HCV infection show diminished NK and NKT cell responses (12–14). In the case of an LT, it has recently been reported that the host CD56$^+$ innate lymphocyte population,

Conflict of interest: The authors have declared that no conflict of interest exists.
Citation for this article: *J. Clin. Invest.* **119**:3226–3235 (2009). doi:10.1172/JCI38374.

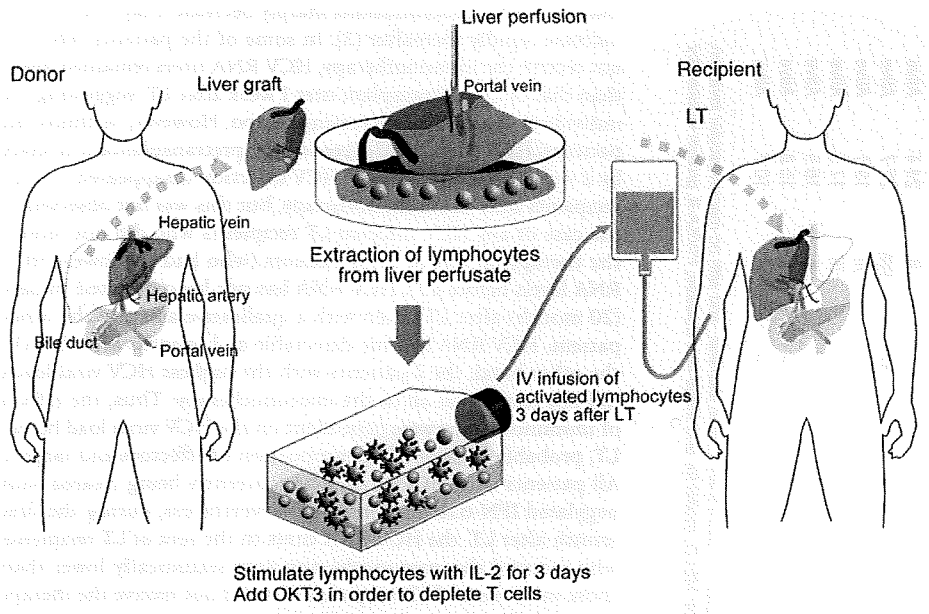

Figure 1
Schematic outline of adoptive immunotherapy with lymphocytes extracted from liver allograft perfusate. The therapy involved giving an intravenous injection of IL-2/OKT3–treated liver lymphocytes to LT recipients. The lymphocytes were extracted from the donor liver graft perfusate. After 3 days of culture with IL-2 (100 JRU/ml), the activated liver NK cell–enriched lymphocytes were administered to the LT recipients through venous circulation. OKT3 (1 μg/ml) was added to the culture medium 1 day before this administration in order to prevent GVHD.

consisting of NK and NKT cells, is appreciably associated with the severity of HCV recurrence after LT (15). These insights into the immunopathogenesis of HCV recurrence indicate that the innate immune components mentioned above are potential targets for therapeutic manipulation. In this study, we have demonstrated for the first time to our knowledge that adoptive immunotherapy with IL-2/OKT3–treated liver lymphocytes, including abundant NK and NKT cells, shows anti-HCV activity after LT, even in an immunosuppressive environment.

Results

Adoptive transfer of IL-2/OKT3–treated liver lymphocytes. The human liver contains a significant number of resident lymphocytes. These cells include abundant $CD56^+$ NK and NKT cells, many of which differ phenotypically and functionally from the circulating cells (14, 16). In our previous study, we performed ex vivo perfusion of the liver through the portal vein, which was necessary in order to flush blood from the liver graft before implantation. Liver-resident lymphocytes were then extracted from the perfusates (number of lymphocytes extracted from normal liver perfusates, 0.5 ± 0.1 cells per gram of liver weight; $n = 14$) (5). Proportions of $CD56^+CD3^-$ NK cells and $CD56^+CD3^+$ NKT cells among the lymphocytes extracted from the liver perfusates (NK cells, 46.4% ± 4.2%; NKT cells, 17.2% ± 2.3%; $n = 14$) were significantly ($P < 0.05$) higher than those among the lymphocytes derived from the peripheral blood of the same donors (NK cells, 21.9% ± 3.7%; NKT cells, 3.8% ± 0.9%; $n = 14$). Extensive preclinical studies have shown that liver allograft–derived resident NK cells mediate remarkably higher cytotoxic activity against HCC cells than do peripheral blood NK cells (5). On this basis, we undertook a clinical trial of adjuvant immunotherapy with IL-2/OKT3–treated liver lymphocytes for preventing the recurrence of HCC after LT in 14 recipients with HCC (Figure 1 and Tables 1 and 2). The therapy involved administering a single intravenous injection of IL-2/OKT3–treated liver lymphocytes to recipients 3 days after LT ($2–5 \times 10^8$ cells injected per subject). In order to prevent graft-versus-host disease (GVHD), i.e., to inactivate $CD3^+$ alloreactive T cells, we added an anti-CD3 mAb, OKT3, to the culture medium a day before the inoculation. During the follow-up period (mean, 23.4 months; range, 10.7–32.9 months), neither any remarkable adverse effects nor rejection episodes occurred. All 14 subjects who received the immunotherapy were alive without recurrence of HCC after LT (including 5 patients with HCC exceeding the Milan criteria; ref. 17). At our institute, the survival rate and recurrence rate of historical control patients with HCC exceeding the Milan criteria were 78% (30 of 37) and 10.8% (4 of 37), respectively. The lymphocytes in the peripheral blood of LT recipients who received immunotherapy in the early postoperative period showed significantly enhanced cytotoxicity against an HCC cell line (HepG2) as compared with those in the peripheral blood of LT recipients who did not receive the therapy in the same period (Figure 2A). Although the gross proportions of NK/NKT cells in the peripheral blood of patients treated with immunotherapy did not differ from those in the peripheral blood of untreated patients, the proportions of $TRAIL^+$ NK cells significantly increased after immunotherapy in the peripheral blood of the former patients. This increase in the $TRAIL^+$ NK cells in the peripheral blood lymphocytes was not observed in untreated patients (Figure 2B). Furthermore, there was a significant correlation between the frequency of $TRAIL^+$ NK cells in the peripheral blood lymphocytes and the NK cytolytic activity of the peripheral blood lymphocytes at 7 days after LT (Spearman rank-order correlation coefficient = 0.54, $P = 0.01$; Figure 2C), indicating the anti-HCC effect of adoptively injected $TRAIL^+$ NK cells. It would be pertinent to conduct additional clinical trials of this immunotherapy for preventing HCC recurrence after LT.

Anti-HCV activity after adoptive immunotherapy. Of the 14 LT recipients who received the immunotherapy, 7 had chronic HCV infection. During the period of this trial, 5 other HCV-infected LT recipients who did not agree to receive immunotherapy served as controls; the background of the controls, including HCV genotype, age, and immunosuppressive therapy, was similar to that of the immunotherapy recipients (Table 3). It has been reported

Table 1
Recipient and tumor characteristics

Patient no.	Age (yr)	Sex	MELD	Hepatitis virus infection	HLA A	HLA B	HLA C	Milan criteria	AFP (ng/ml)	PIVKA-II (AU/ml)	Tumor no.	Maximum tumor size (mm)	Path. vascular invasion	Path. stage	Postop. months	Outcome
1	67	M	19	B	24,-	13,40	03,-	OUT	–	2,584	5	35	–	III	32 9	Alive
2	53	M	16	B	2603,3303	4002,4403	0304,1403	IN	25 3	43	4	11	–	II	31 0	Alive
3	54	M	7	B	0206,3101	3501,5101	0303,1402	OUT	5 7	213	11	26	–	III	29 4	Alive
4	64	F	16	C	2601,2603	3501,4801	0303,-	IN	5 9	142	–	–	–	–	28 5	Alive
5	59	F	14	B	0206,2601	4002,5502	0102,0304	OUT	<5	65	1	13	b1	II	27 8	Alive
6	47	F	8	C	2402,2601	3501,5201	0303,1202	IN	18	46	3	12	–	II	26 2	Alive
7	57	M	29	B	2402,3101	5101,5201	1202,1402	IN	40.3	514	1	25	–	II	25 4	Alive
8	65	F	18	C	1101,2402	5401,5901	0102,-	IN	–	–	3	6	–	II	24 4	Alive
9	60	F	8	–	1101,3001	1302,4006	0602,0801	OUT	32 8	3,026	2	40	vv1	IVA	22 7	Alive
10	56	M	8	C	2402,3303	5201,5801	0302,1202	OUT	–	304	11	22	–	III	19 1	Alive
11	56	M	9	C	0207,-	4601,-	0102,-	IN	47	20	3	25	–	III	17 5	Alive
12	58	M	22	C	1101,3101	1501,3501	0102,0415	IN	–	62	1	17	–	I	16 5	Alive
13	59	M	6	C	1101,2402	1507,1501	0303,0401	IN	202 9	19	3	16	–	II	15 8	Alive
14	51	M	16	B	1101,2601	4002,5401	0102,0304	IN	–	29	–	–	–	–	10 7	Alive

The Milan criteria specifies that liver cancer patients with a single tumor of 5 or fewer centimeters in diameter or 3 or fewer tumors, each no more than 3 cm in diameter, and with no macrovascular invasion, can expect an excellent outcome after LT, with only a 10% risk of cancer recurrence (31). AFP, alpha fetoprotein; F, female; M, male; MELD, model for end-stage liver disease; PIVKA-II, protein induced by vitamin K absence; Path., pathological; Postop., postoperative.

that HCV RNA concentrations sharply decrease a day after LT and increase rapidly thereafter (3). In some of the patients, who did not receive the immunotherapy, HCV RNA titers remained lower than that of the pretransplant titer 1 week after LT, suggesting the individual variation of increasing tempo. However, in almost all patients, HCV RNA titers exceeded the pretransplantation levels by 2 weeks after LT. Notably, HCV infection disappeared in 2 LT recipients after the immunotherapy, but this was not observed in the case of any HCV-infected LT recipients who did not receive the therapy. In one of these patients (who had the lowest HCV RNA levels before LT), HCV RNA has not been detected to date (20 months after LT), even with a qualitative assay. In the other patient, HCV RNA became detectable at 2 months after LT. On the other hand, the 2 patients with the highest HCV viral loads did not respond at all to the immunotherapy. Thus, the effects of immunotherapy were dependent on the HCV virus load before LT, probably because of the proportion of effectors and targets. All patients with HCV viremia are currently being treated with pegylated IFN-α2b and ribavirin. Nevertheless, during the first month after LT, the HCV RNA titers in the sera of LT recipients who received the immunotherapy were statistically lower than those in the sera of LT recipients who did not receive the therapy ($P < 0.05$) (Figure 3). Among the LT recipients who received the immunotherapy, at 2 weeks after LT, HCV RNA remained undetectable in 4 patients (responders), whereas it was detectable in the other 3 patients (nonresponders). The serum ALT levels did not differ between the responders and nonresponders (Supplemental Figure 1; supplemental material available online with this article; doi:10.1172/JCI38374DS1), suggesting that the immunotherapy did not inhibit HCV RNA by injuring HCV-infected hepatocytes.

In vitro evidence to prove the anti-HCV activity of IL-2/OKT3–treated liver lymphocytes by using HCV replicon–containing hepatic cells. The liver allograft–derived lymphocytes were cultured in complete medium with and without IL-2 for 3 days. This was followed by adding OKT3 to the culture medium 1 day before coculturing the lymphocytes with HCV replicon–containing hepatic cells in a transwell system, at an indicated time. While the freshly isolated liver allograft–derived lymphocytes inhibited HCV replication in the HCV replicon–containing hepatic cells to some extent, the cultivation of these lymphocytes with IL-2/OKT3 markedly promoted anti-HCV activity. Absence of exposure to either IL-2 or OKT3 resulted in reduced anti-HCV activity of the lymphocytes (OKT3 had a more profound influence than IL-2) (Figure 4A). When the lymphocytes were treated with IL-2 alone, the $CD56^+$ fraction, including NK and NKT cells, that had been isolated by magnetic cell sorting inhibited HCV replication more strongly than the $CD56^-$ fraction; further, the $CD3^-CD56^+$ NK cell and $CD3^+CD56^+$ NKT cell subfractions showed equivalent anti-HCV activity (Figure 4, B and C). On the other hand, when the lymphocytes were treated with both IL-2 and OKT3, the $CD56^+$ and $CD56^-$ fractions showed similar levels of anti-HCV activity (Figure 4B). After the treatment with IL-2 and OKT3, IFN-γ was the predominant cytokine in the culture supernatant of the lymphocytes (Figure 5A), and intracellular IFN-γ expression was induced in the $CD3^-CD56^+$ NK, $CD3^+CD56^-$ NKT, and $CD3^+CD56^-$ T cells (Figure 5B). There was no difference between the proportions of $TRAIL^+$ and $TRAIL^-$ $CD3^-CD56^+$ NK cells producing IFN-γ (Supplemental Figure 2). Adding mAb against IFN-γ to the coculture of lymphocytes with HCV replicon cells markedly weakened the anti-HCV effects. The incomplete restoration of the anti-HCV effect by anti–IFN-γ treat-

Table 2
Donor and graft characteristics

Donor no.	Donor age (yr)	Donor sex	HLA A	HLA B	HLA C	Relationship	Graft	Graft weight (g)	No. of cells administered ($\times 10^6$)
1	41	M	24,-	07,40	03.07	Offspring	Right	608	172
2	24	M	2402,2603	4002,2603	0304,5201	Offspring	Right	658	38
3	51	F	0201,2402	0702,3901	0702,-	Spouse	Right	670	129
4	34	M	2601,2603	4001,4801	0303,0401	Offspring	Left	414	143
5	31	M	0206,2402	4002,5401	0102,0304	Offspring	Posterior	702	135
6	53	F	2402,-	5201,5401	0102,1202	Sibling	Right	538	411
7	24	M	2601,3101	4006,5201	0801,1202	Offspring	Right	642	350
8	34	M	1101,-	4001,5401	0102,1502	Offspring	Right	846	229
9	37	M	0201,1101	1501,4006	0702,0801	Offspring	Left	402	811
10	28	M	1101,3303	5502,5801	0102,0302	Offspring	Right	686	517
11	28	M	0207,2402	4601,5201	0102,5201	Offspring	Right	558	414
12	27	M	0201,1101	1501,3501	0303,0415	Offspring	Right	628	509
13	54	F	1101,2402	1501,1507	0303,0401	Sibling	Right	650	460
14	21	F	2601,2603	1501,5401	0102,0303	Offspring	Right	436	382

ment suggests the possibility that other inflammatory cytokines may also be responsible for the anti-HCV effect, although we have not defined them at present (Figure 5C). Thus, the vigorous anti-HCV activity of IL-2/OKT3–treated liver lymphocytes was dependent, at least in part, on their IFN-γ–secreting activity.

IFN-γ–secreting activity in LT recipients after adoptive immunotherapy. At 14 days after LT, the number of IFN-γ–secreting cells in the peripheral blood of LT recipients who received adoptive immunotherapy was significantly higher than that in the peripheral blood of LT recipients who did not receive immunotherapy during the trial period (Figure 6). This result was consistent with the results of the in vitro studies showing the crucial role of IFN-γ produced in IL-2/OKT3–treated liver lymphocytes.

In vivo evidence to prove the anti-HCV activity of adoptive immunotherapy by using HCV-infected human hepatocyte–chimeric mice. HCV-infected mice have previously been developed by inoculating HCV-infected human serum into chimeric urokinase-type plasminogen activator–SCID (uPA-SCID) mice with engrafted human hepatocytes (18). This HCV-infected mouse model has been reported to be useful for evaluating anti-HCV drugs such as IFN-α and anti-NS3 protease (19). We also generated a human hepatocyte–chimeric mouse model, in which mouse hepatocytes were almost completely replaced by human hepatocytes (20). These mice consistently developed long-term HCV infections, showing high viral titers after inoculation with HCV genotype 1b–infected human serum (50 μl/mouse) (Supplemental Figure 3). Intraperitoneal injection of IL-2/OKT3–treated liver lymphocytes (20×10^6 cells/mouse), at 2 weeks after inoculation with the infected serum, consistently prevented the development of HCV infection in the human hepatocyte–chimeric mice (Figure 7A). Such anti-HCV effects were countered by anti–IFN-γ neutralizing antibodies in some chimeric mice, suggesting the potential role played by IFN-γ in the anti-HCV effects of the immunotherapy. The administration of recombinant human IFN-γ markedly and consistently prevented the development of HCV infection in the human hepatocyte–chimeric mice. Once the HCV RNA became undetectable in the sera of chimeric mice receiving either IL-2/OKT3–treated liver lymphocytes or recombinant IFN-γ, it could not be detected again. The constant levels of human serum albumin in the chimeric mice indicated that neither the immunotherapy nor recombinant IFN-γ administration had significant adverse effects on human hepatocytes in those mice (Figure 7B). Once HCV infection had developed in the human hepatocyte–chimeric mice, who showed high titers of HCV RNA in their sera (over 10^3 copies/ml) 4 weeks after the inoculation of HCV-infected serum, the preventive effects of the adoptive immunotherapy or recombinant IFN-γ on HCV infection were no longer observed (Figure 7C).

Table 3
Characteristics of HCV-infected LT recipients that received and did not receive immunotherapy

No.	Age	Sex	HCV genotype	MELD	Pre–HCV RNA (KIU/ml)	Postoperative months	Immunosuppressant
With immunotherapy							
4	64	F	1b	16	210	29	Basiliximab+FK506+MMF
6	47	F	1b	8	5,000	26	Basiliximab+CsA+MMF
8	65	F	1b	18	2,400	24	Basiliximab+CsA+MMF
10	56	M	1b	8	970	19	Basiliximab+FK506+MMF
11	56	M	1b	9	1,700	17	Basiliximab+FK506+MMF
12	58	M	1b	22	19	17	Basiliximab+FK506+MMF
13	59	M	1b	6	2,200	16	Basiliximab+FK506+MMF
Without immunotherapy							
A	51	M	1b	27	420	42	Basiliximab+FK506+MMF
B	44	M	1b	10	1,600	32	Basiliximab+FK506+MMF
C	54	M	1b	8	180	22	Basiliximab+CsA+MMF
D	56	M	2a	10	470	20	Basiliximab+FK506+MMF
E	57	M	1b	12	3,200	6	Basiliximab+FK506+MMF

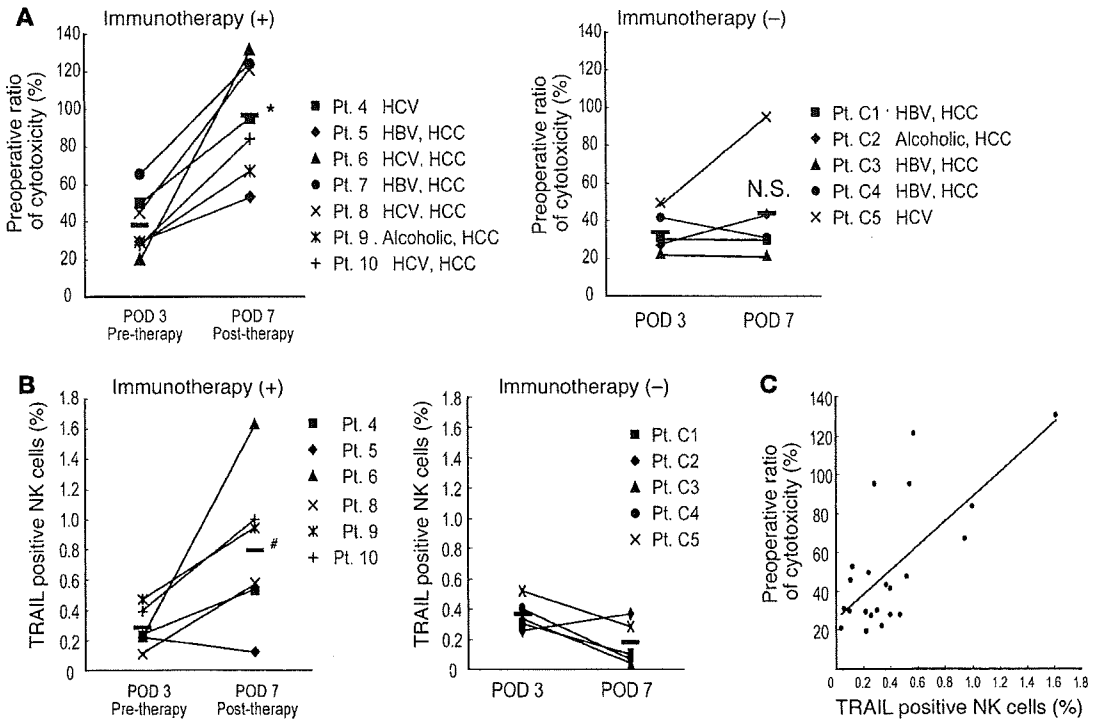

Figure 2

Adoptive immunotherapy with IL-2/OKT3–treated liver lymphocytes promoted the cytotoxic activity and TRAIL expression of NK cells in LT recipients. (**A**) The NK cytotoxic activities of the indicated effectors against their target cells were analyzed by the ^{51}Cr-release assay. The dot plot represents the NK cytotoxic activities of freshly isolated peripheral blood lymphocytes obtained from recipients who received immunotherapy (+) ($n = 7$) and did not receive immunotherapy (–) ($n = 5$) against HepG2 target cells (effector/target [E/T] ratio, 40:1) 3 and 7 days after LT. NK cytotoxic activities are represented as a proportion (percentage) of the preoperative cytotoxicity in each patient. Horizontal lines indicate the mean. Statistical analyses were performed using the 2-tailed, paired Student's t test. $^{*}P < 0.05$ for day 7 versus day 3. (**B**) The frequency of TRAIL^{+} NK cells increased remarkably in the peripheral blood of LT recipients who received the immunotherapy. Horizontal lines indicate the mean. Statistical analyses were performed using the Mann-Whitney U test. $^{\#}P = 0.013$ for immunotherapy group versus untreated group in postoperative day 7. (**C**) Correlation between TRAIL^{+} NK cell ratio and NK cytolytic activity after LT (Spearman rank-order correlation coefficient = 0.54, $P = 0.01$). Statistical analyses were performed using the Spearman rank-order correlation coefficient. The diagonal line indicates a linear regression line. Each dot indicates the cytotoxicity and TRAIL^{+} NK cell percentange of each patient. C1, control 1; POD, postoperative day; Pt., patient.

Discussion

The consequences of recurrent hepatitis C on the survival of graft and LT recipients can only be avoided by the development of safe and effective antiviral strategies that can not only prevent initial graft infection but also eradicate established hepatitis C recurrence (3, 4). With regard to initial graft infection, the circulating virions infect the liver graft immediately after LT. HCV RNA concentrations usually increase a few days after LT, reflecting active HCV replication in the liver graft. In general, in such an early phase of a viral infection, the first line of host defense may be effective in removing the virus; however, recent reports have indicated that HCV effectively escapes the innate immune system comprising NK and NKT cells, resulting in persistent infection (21, 22). It has been reported that cross-linking of CD81 on NK cells by the major envelope protein of HCV, HCV-E2, blocks NK cell activation, IFN-γ production, cytotoxic granule release, and proliferation (21). Engagement of CD81 on NK cells blocks tyrosine phosphorylation through a mechanism that is distinct from the negative signaling pathways associated with NK cell inhibitory receptors for major histocompatibility complex class I molecules (22). These facts prove that HCV-E2–mediated inhibition of NK cells is an efficient HCV evasion strategy, which involves targeting the early antiviral activities of NK cells and allowing the virus to establish itself as a chronic infection.

We have explored whether CD81 cross-linking–induced inhibitory effects occur even in IL-2–stimulated NK cells. CD81 cross-linking by a mAb specific for CD81 inhibited antitumor cytotoxicity and anti-HCV activity mediated by resting NK cells, but this manipulation did not alter both these activities of IL-2–stimulated NK cells (Supplemental Figure 4). This indicated that exposure to IL-2 before CD81 cross-linking abrogates subsequent inhibitory signals in the NK cells. This would be one mechanism whereby the adoptive immunotherapy with IL-2/OKT3–treated liver lymphocytes inhibited HCV replication at the early phase of infection after LT.

Although the role of NK cells in controlling HCV infection and replication has not been completely elucidated, a recent report has indicated that NK cells do not exert a direct cytolytic effect on the HCV replicon–containing hepatic cells but release IFN-γ, suppressing HCV RNA expression (11). The role of IFN-γ in the expression of NK cell–mediated anti-HCV activity has been proved by the observa-

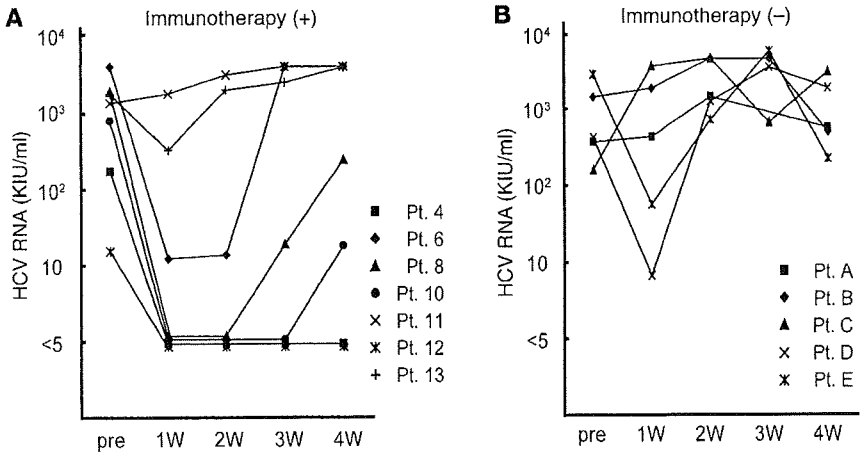

Figure 3
Serial measurement of the HCV RNA titers of LT recipients after LT The HCV RNA titers in the sera of LT recipients who received immunotherapy were markedly lower than those in the sera of LT recipients who did not receive the therapy during the first month after LT Each line with a different symbol represents serial HCV RNA titers from an LT recipient who received (+) (**A**; $n = 7$) and 1 who did not receive (–) (**B**; $n = 5$) the immunotherapy after LT KIU, kilo international unit; pre, pre LT, W, week.

tion that NK cell–conditioned media have an enhanced expression of signal transducer and activator of transcription 1, a nuclear factor that is essential in IFN-γ–mediated antiviral pathways. It has also been reported that hepatocytes cultured in NK cell–conditioned media express higher levels of IFN-α/β, IFN regulatory factor 3, and IFN regulatory factor 7, confirming that NK cells play a key role in suppressing HCV infection of and replication in human hepatocytes in an IFN-dependent manner (23). Similar to recent reports, in the present study, we demonstrated that the NK cells among the IL-2/OKT3–treated liver lymphocytes released soluble factors, predominantly IFN-γ, thus suppressing HCV replication (Figures 5–7).

In addition to NK cells, NKT cells are thought to be involved in eliciting innate responses against infection; however, the role of NKT cells in controlling HCV infection/replication remains unclear. One report has indicated that the number of NKT cells in patients with chronic HCV infection does not differ from that in healthy donors; however, activated NKT cells in HCV-infected patients produce higher levels of IL-13 — but comparable levels of IFN-γ — than those in healthy subjects, showing that NKT cells are biased toward T-helper 2-type responses in chronic HCV infection (24). Another recent report has shown that the sustained response of patients with chronic hepatitis C to treatment with IFN-α and ribavirin is closely associated with increased dynamism of NK and NKT cells in the liver, implicating an NKT cell–mediated mechanism in anti-HCV activity (25). Here, we have described that NKT as well as NK cells in the IL-2/

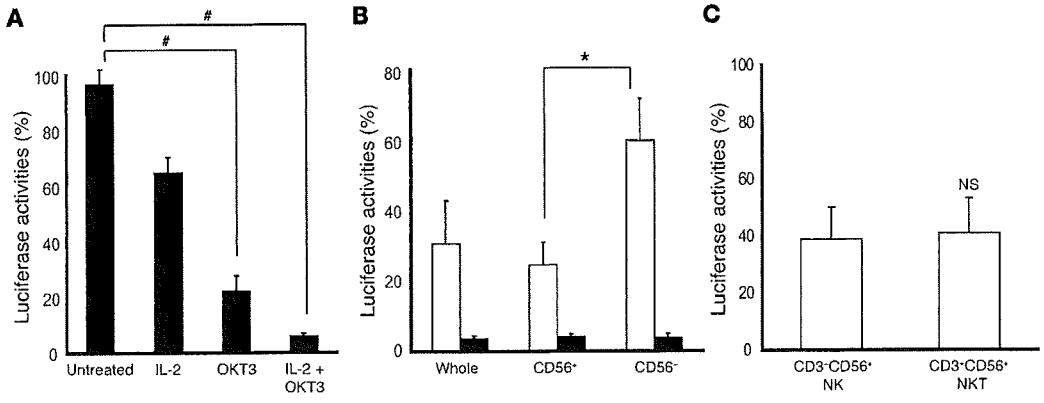

Figure 4
The cultivation of liver lymphocytes with IL-2/OKT3 markedly promoted anti-HCV activity. (**A**) Activation by IL-2 and OKT3 significantly promoted the anti-HCV effect of the liver allograft–derived lymphocytes that were cultured in complete medium with and without IL-2 (100 JRU/ml) for 3 days. OKT3 (1 μg/ml) was then added 1 day before coculturing with HCV replicon cells, at the indicated time. The bar graphs indicate the luciferase activities of the cells in each group. Data are presented as mean ± SEM ($n = 5$). Statistical analyses were performed using the Mann-Whitney *U* test with Bonferroni correction after the Kruskal-Wallis *H* test. $^{\#}P < 0.01$ for OKT3 and IL-2/OKT3 treatment versus no treatment. (**B**) $CD56^+$ fraction, including NK and NKT cells, strongly inhibited HCV replication. The culture conditions are described in **A**. By magnetic cell sorting, $CD56^+$ and $CD56^-$ fractions were isolated from the activated lymphocytes and analyzed for anti-HCV activity. The bar graphs indicate the luciferase activities of the cells in each group (IL-2–treated group, white bars; IL-2 plus OKT3–treated group, black bars). Whole, whole lymphocytes. Data are presented as mean ± SEM ($n = 5$). Statistical analyses were performed using the Mann-Whitney *U* test. $^*P < 0.05$ for $CD56^+$ fraction versus $CD56^-$ fraction. (**C**) Anti-HCV effect of NK cells was almost identical to that of NKT cells after IL-2 activation. The liver allograft–derived lymphocytes were cultured in complete medium with IL-2 (100 JRU/ml) for 3 days. By magnetic sorting, $CD3^-CD56^+$ (NK) and $CD3^+CD56^+$ (NKT) fractions were isolated from the activated lymphocytes and analyzed for anti-HCV activity. Data are presented as mean ± SEM ($n = 6$).

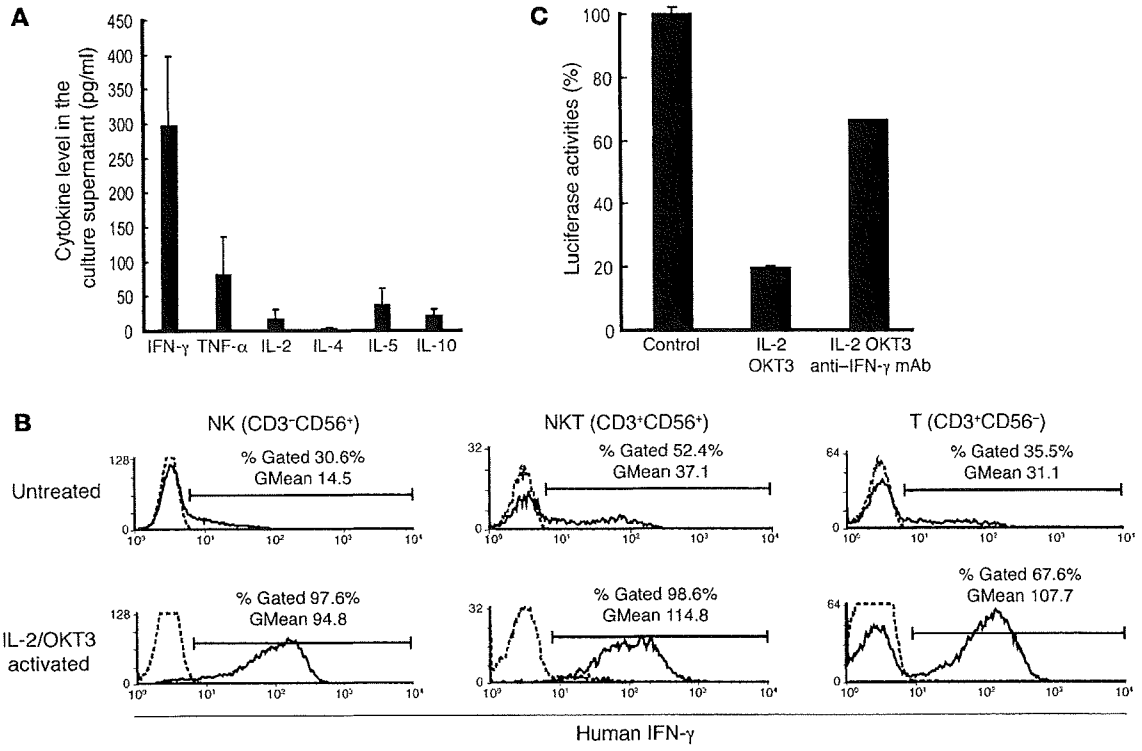

Figure 5

Anti-HCV activity of IL-2/OKT3–treated liver lymphocytes was dependent on their IFN-γ secretion ability. (**A**) IFN-γ was the major cytokine released from the cultured cells. The bar graphs indicate the concentrations of various cytokines (IFN-γ, TNF-α, IL-2, IL-4, IL-5, and IL-10) detected in the coculture supernatant by CBA. Data are presented as mean ± SEM (n = 3). (**B**) The effects of IL-2 and OKT3 (100 JRU/ml and 1 μg/ml, respectively) on IFN-γ production by stimulated $CD3^-CD56^+$ NK, $CD3^+CD56^+$ NKT, and $CD3^+CD56^-$ T cells were evaluated by a combination of cell surface and cytoplasmic mAb staining and subsequent flow cytometric analysis. Histograms represent the log fluorescence intensities obtained upon staining for IFN-γ after gating of each fraction. Dotted lines represent negative control staining with isotype-matched mAbs. Horizontal lines indicate the gated portion of lymphocytes. GMean, geometric mean fluorescent intensity. (**C**) Blocking of IFN-γ with mAb (100 μg/ml) elucidated the marked role played by IFN-γ in producing the anti-HCV effect. The bar graphs indicate the luciferase activities of the cells in each group. Data are presented as mean ± SEM of a representative triplicate sample.

OKT3-treated liver lymphocytes could play a vital role in controlling HCV replication in hepatic cells via an IFN-γ–associated mechanism (Figures 5 and 6).

Therefore, in the early phase of HCV reinfection after LT, the effects of IFN-γ secretion from adoptively injected liver lymphocytes may include inhibition of HCV virion production, which is probably caused by suppression of viral RNA and protein synthesis without immune lysis of intact hepatic cells. This IFN-γ secretion from both $CD3^+CD56^-$ NKT cells and $CD3^+$ T cells was markedly upregulated after treatment with OKT3, which was originally used to prevent GVHD (Figure 5B). This is possibly because of the potent mitogenic activity of OKT3 that induces the activation of $CD3^+CD56^+$ NKT cells and $CD3^+$ T cells. However, the administration of OKT3-coated cells in vivo results in the opsonization and subsequent trapping and/or lympholysis of cells by the reticuloendothelial system (26–28). Thus, GVHD is prevented in LT recipients treated with adoptive immunotherapy.

Our finding that the IL-2/OKT3-treated liver lymphocytes controlled HCV replication via an IFN-γ–associated mechanism can lead to the clinical application of recombinant IFN-γ for anti-HCV treatment. However, a clinically applicable dose of recombinant IFN-γ could not induce significant inhibitory effects on HCV viremia in the previous study (29). Based on the accumulation of adoptively injected IL-2/OKT3-treated liver lymphocytes in the liver of human hepatocyte-chimeric mice (data not shown), the immunotherapy with the liver lymphocytes would provide sufficient IFN-γ to the HCV-infected site.

It has been recently reported that HCV-specific $CD8^+$ T cells exert strong antiviral effects by both cytopathic and IFN-γ–mediated noncytopathic effector functions (30). However, in patients with chronic HCV infection, dysfunction and functional restoration of HCV-specific $CD8^+$ T cell responses have been reported (31). Since HCV-specific $CD8^+$ T cell defects may be important in persistent HCV infections, correcting these defects is considered to our knowledge to be a novel approach to treat HCV infection. Further studies are required to investigate whether activation of NK or NKT cells functionally restores HCV-specific $CD8^+$ T cells.

In conclusion, adoptive immunotherapy using IL-2/OKT3-treated liver lymphocytes containing abundant NK and NKT cells could mount remarkable anti-HCV responses in HCV-infected LT recipients, although its effects were incomplete or transient. Treatment-related improvements, such as defining the best schedule and frequency of cell inoculation and developing more potent effectors, could improve clinical benefits.

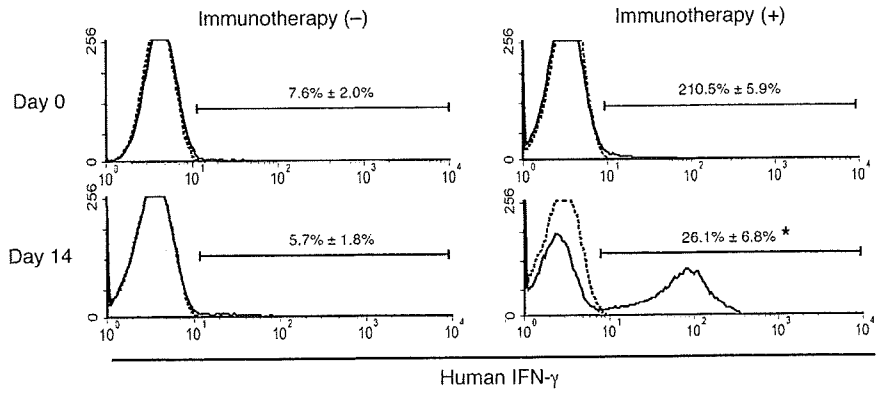

Figure 6
Adoptive immunotherapy with IL-2/OKT3–treated liver lymphocytes induced the production of IFN-γ in the LT recipients. At 14 days after LT, the number of IFN-γ–secreting cells in the peripheral blood of LT recipients treated with the adoptive immunotherapy (+) with IL-2/OKT3–treated liver lymphocytes, including NK and NKT cells, was significantly higher than that in the peripheral blood of untreated LT recipients (–). Histograms represent the proportion (percentage) of IFN-γ–positive cells among the mononuclear cells obtained from the peripheral blood of the immunotherapy (n = 4) and control group (n = 4) LT recipients. Dotted lines represent negative control staining with isotype-matched mAbs. Horizontal lines indicate the gated portion of lymphocytes. Data are presented as mean ± SEM. Histogram profiles shown are representative of 4 independent experiments. Statistical analyses were performed using the Mann-Whitney U test. *$P < 0.05$ for immunotherapy group versus control group.

Methods

Subjects. All the human liver samples were collected at Hiroshima University Hospital. Tissue specimens were collected after approval from the Institutional Review Board of Hiroshima University and after written informed consent was obtained from the patients. The use of immunotherapy with IL-2/OKT3–treated liver lymphocytes was approved by the Clinical Institutional Ethical Review Board of Hiroshima University. Written informed consent was obtained from all of the patients. This approach was successfully used in 14 cirrhotic patients with HCC undergoing clinical LT (Tables 1 and 2). Of these 14 patients, 7 had chronic HCV infection. Five other LT recipients with chronic HCV infection did not agree to receive this immunotherapy during the trial period. HCV RNA was qualitatively detected in the sera of these patients by a standardized qualitative RT-PCR assay (Amplicor HCV monitor, version 2.0; Roche Diagnostics) every week during the first month after LT.

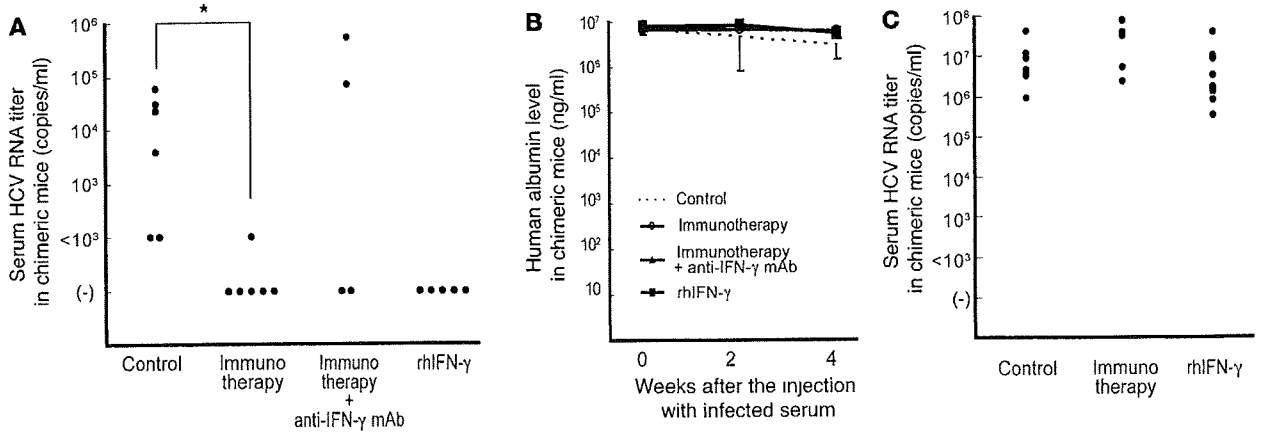

Figure 7
Adoptive immunotherapy with IL-2/OKT3–treated liver lymphocytes prevented HCV infection in human hepatocyte–chimeric mice. (**A**) Human hepatocyte–chimeric mice were intravenously injected with human serum samples positive for HCV genotype 1b. Two weeks after injecting the infected serum, the mice were intraperitoneally inoculated with IL-2/OKT3–treated liver lymphocytes (20 × 10^6 cells/mouse; n = 6) for adoptive immunotherapy. When indicated, anti-human IFN-γ mAb was injected intraperitoneally 1 day before the immunotherapy (n = 4). Intraperitoneal injection of recombinant human IFN-γ (rhIFN-γ) was commenced at 2 weeks after injecting the infected serum (n = 5). The untreated mice served as controls (n = 6). The dot plots represent serum HCV RNA titers in each chimeric mouse 4 weeks after the injecting the infected serum. Statistical analyses were performed using the Mann-Whitney U test. *$P < 0.01$ for immunotherapy group versus control group. (**B**) The lines represent serial changes in human serum albumin levels in the sera of the mice indicated above. Data are presented as mean ± SEM. (**C**) IL-2/OKT3–treated liver lymphocytes (20 × 10^6 cells/mouse) were intraperitoneally inoculated 4 weeks after the injection with the infected serum (n = 5) for adoptive immunotherapy. Intraperitoneal injection of recombinant human IFN-γ was commenced 4 weeks after the injecting the infected serum (n = 9). The untreated mice served as controls (n = 9). The dot plots represent serum HCV RNA titers in each chimeric mouse 6 weeks after injection with the infected serum.

Isolation of lymphocytes from liver allograft perfusate. Donor hepatectomy and the transplantation procedure were performed as described previously (32). After hepatectomy, ex vivo perfusion of the liver allograft was performed through the portal vein. Liver allograft–derived lymphocytes were isolated by gradient centrifugation with Ficoll-Paque (GE Healthcare Bio-Sciences AB).

Adoptive transfer of IL-2/OKT3–treated liver lymphocytes. Liver lymphocytes were cultured with human recombinant IL-2 (100 Japanese reference units/ml [JRU/ml]; Takeda) in complete medium at 37°C in a 5% CO_2 incubator for 3 days. One day before the infusion, 1 μg/ml of OKT3 (Janssen-Kyowa) was added in order to opsonize the $CD3^+$ fraction. On the day of infusion, the cells were washed twice with 0.9% sodium chloride and resuspended with 5% human serum albumin in 0.9% sodium chloride for injection (Figure 1). The viability of the cells was assessed by the dye-exclusion test, and the cells were checked twice for possible contamination by bacteria, fungi, and endotoxins.

Cytotoxicity assay. A ^{51}Cr-release assay was done as previously described (5), using HepG2 tumor cells (Japanese Cancer Research Resources Bank) as targets. Briefly, ^{51}Cr-labeled target tumor cells were added for 4 hours at 37°C to effector cells in round-bottomed 96-well microtiter plates (BD Biosciences — Discovery Labware). The percentage of specific ^{51}Cr release was calculated as follows: % cytotoxicity = [(cpm of experimental release − cpm of spontaneous release)/(cpm of maximum release − cpm of spontaneous release)] × 100. All the assays were performed in triplicate.

Flow cytometry. Flow cytometric analyses were performed using a FACSCalibur dual-laser cytometer (BD Biosciences). The following mAbs were used for the surface staining of the lymphocytes: FITC-conjugated anti-CD3 mAb (clone HIT3a; BD Biosciences — Pharmingen); PE-conjugated anti-CD56 mAb (clone B159; BD Biosciences — Pharmingen); and biotinylated anti-TRAIL (biotin-conjugated anti-TRAIL) mAb (clone RIK-2; eBioscience). The biotinylated mAb was visualized using APC-streptavidin (BD Biosciences — Pharmingen). Dead cells identified by light scatter and propidium iodide staining were excluded from the analysis. IFN-γ production in the lymphocytes was measured by a combination of cell surface and cytoplasmic mAb staining and subsequent flow cytometric analysis, as described previously (33).

Isolation of $CD56^+$ and $CD56^-$ fractions and that of NK and NKT cells. Liver allograft–derived lymphocytes were separated into a $CD56^+$ fraction — including NK and NKT cells — and a $CD56^-$ fraction by using auto MACS (Miltenyi Biotec) with anti-human CD56 microbeads (Miltenyi Biotec) according to the manufacturer's instructions. The NK and NKT cells were also isolated by magnetic cell sorting, using the human NK cell isolation kit or human $CD3^-CD56^+$ NKT cell isolation kit (Miltenyi Biotec). The purity of the isolated fractions was assessed by flow cytometric analysis, and only the fractions with purities greater than 90% were used for functional studies.

Coculture with HCV replicon–containing hepatic cells. An HCV subgenomic replicon plasmid, pRep-Feo, was derived from pRep-Neo (originally, pHCVIbneo-delS; ref. 34). The pRep-Feo carries a fusion gene comprising firefly luciferase (*Fluc*) and neomycin phosphotransferase, as described elsewhere (35, 36). After culture in the presence of G418 (Invitrogen), pRep-Feo cell lines stably expressing the replicons were established. For coculture experiments, transwell tissue culture plates (pore size, 1 μm; Costar) were used. HCV replicon–containing hepatic cells (10^5 cells) were incubated in the lower compartment with different numbers of lymphocytes in the upper compartment. The hepatic cells in the lower compartments were collected 48 hours after coculture for the luciferase assay. Luciferase activities were measured with a luminometer (Lumat LB9501; Promega), using the Bright-Glo Luciferase Assay System (Promega).

Cytometric bead array. Cytokine (IFN-γ, TNF-α, IL-2, IL-4, IL-5, IL-10) levels in the coculture assay supernatants were measured with the FACSCalibur dual-laser cytometer (BD Biosciences), using a BD Human Th1/Th2 Cytokine Cytometric Bead Array (CBA) Kit according to the manufacturer's instructions.

Generation of human hepatocyte–chimeric mice. Generation of the *uPA*$^{+/+}$ *SCID*$^{+/+}$ mice and transplantation of human hepatocytes were performed as described recently by our group (20, 37). Mouse serum concentrations of human serum albumin correlated with the repopulation index (20), and these were measured as described previously (37).

In vivo studies using human hepatocyte–chimeric mice. Human hepatocyte-chimeric mice were intravenously injected with 50 μl of the human serum samples positive for HCV genotype 1b. The serum HCV RNA titer in human hepatocyte-chimeric mice was detected by nested PCR, as previously described (38, 39). All animal protocols described in this study were performed in accordance with the guidelines and with approval of the Ethics Review Committee of Animal Experimentation of the Graduate School of Biomedical Sciences, Hiroshima University. Either 2 or 4 weeks after injecting the infected serum, the mice were intraperitoneally inoculated with IL-2/OKT3–treated liver lymphocytes (20×10^6 cells/mouse) for adoptive immunotherapy. When indicated, anti-human IFN-γ mAb (R&D Systems) (1.5 mg/mouse) was injected intraperitoneally 1 day before the immunotherapy. In a separate experiment, intraperitoneal injection of recombinant human IFN-γ (Imunomax-γ; Shionogi & Co. Ltd.) was commenced at either 2 or 4 weeks after injecting the infected serum. IFN-γ was administered as follows: 1×10^5 IU on the first day and thereafter 2×10^4 IU/day for 13 days.

Statistics. Data are presented as mean ± SEM. The statistical differences of the results were analyzed by 2-tailed, paired Student's *t* test, Mann-Whitney *U* test, and Mann-Whitney *U* test with Bonferroni correction after the Kruskal-Wallis *H* test, using the Stat View program. *P* values of 0.05 or less were considered statistically significant.

Acknowledgments

This work was supported in part by a Grant-in-Aid for Exploratory Research (19659323) from the Japan Society for the Promotion of Science. We thank Kentaro Ide, Toshimitsu Irei, Hiroyuki Tahara, Masataka Banshodani, Nabin Basnet, Hirofumi Tazawa, and Keiko Kajitani for their advice and encouragement and Yuko Ishida for expert technical assistance.

Received for publication December 17, 2008, and accepted in revised form July 29, 2009.

Address correspondence to: Hideki Ohdan, Department of Surgery, Division of Frontier Medical Science, Programs for Biomedical Research, Graduate School of Biomedical Sciences, Hiroshima University, 1-2-3 Kasumi, Minami-ku, Hiroshima 734-8551, Japan. Phone: 81-82-257-5220; Fax: 81-82-257-5224; E-mail: hohdan@hiroshima-u.ac.jp. Or to: Kazuaki Chayama, Department of Medicine and Molecular Science, Division of Frontier Medical Science, Programs for Biomedical Research, Graduate School of Biomedical Sciences, Hiroshima University, 1-2-3 Kasumi, Minami-ku, Hiroshima 734-8551, Japan. Phone: 81-82-257-5190; Fax: 81-81-257-5194; E-mail: chayama@hiroshima-u.ac.jp.

1. Petrovic, L.M. 2006. Early recurrence of hepatitis C virus infection after liver transplantation. *Liver Transpl.* **12**:S32–S37.
2. Brown, R.S. 2005. Hepatitis C and liver transplantation. *Nature.* **436**:973–978.
3. Garcia-Retortillo, M., et al. 2002. Hepatitis C virus kinetics during and immediately after liver transplantation. *Hepatology.* **35**:680–687.
4. Berenguer, M. 2002. Natural history of recurrent hepatitis C. *Liver Transpl.* **8**:S14–S18.
5. Ishiyama, K., et al. 2006. Difference in cytotoxicity against hepatocellular carcinoma between liver and periphery natural killer cells in humans. *Hepatology.* **43**:362–372.
6. Ohira, M., et al. 2006. Adoptive transfer of TRAIL-

expressing natural killer cells prevents recurrence of hepatocellular carcinoma after partial hepatectomy. *Transplantation.* **82**:1712–1719.
7. Miller, J.S., et al. 2005. Successful adoptive transfer and in vivo expansion of human haploidentical NK cells in patients with cancer. *Blood.* **105**:3051–3057.
8. Hirata, M., et al. 1998. Increase in natural killer cell activity following living-related liver transplantation. *Transpl. Int.* **11**(Suppl. 1):S185–S188.
9. Harada, N., et al. 2004. IL-12 gene therapy is an effective therapeutic strategy for hepatocellular carcinoma in immunosuppressed mice. *J. Immunol.* **173**:6635–6644.
10. Golden-Mason, L., and Rosen, H.R. 2006. Natural killer cells: primary target for hepatitis C virus immune evasion strategies? *Liver Transpl.* **12**:363–372.
11. Li, Y., et al. 2004. Natural killer cells inhibit hepatitis C virus expression. *J. Leukoc. Biol.* **76**:1171–1179.
12. Deignan, T., et al. 2002. Decrease in hepatic CD56(+) T cells and V alpha 24(+) natural killer T cells in chronic hepatitis C viral infection. *J. Hepatol.* **37**:101–108.
13. Durante-Mangoni, E., et al. 2004. Hepatic CD1d expression in hepatitis C virus infection and recognition by resident proinflammatory CD1d-reactive T cells. *J. Immunol.* **173**:2159–2166.
14. Kawarabayashi, N., et al. 2000. Decrease of CD56(+)T cells and natural killer cells in cirrhotic livers with hepatitis C may be involved in their susceptibility to hepatocellular carcinoma. *Hepatology.* **32**:962–969.
15. Rosen, H.R., et al. 2008. Pretransplantation CD56(+) innate lymphocyte populations associated with severity of hepatitis C virus recurrence. *Liver Transpl.* **14**:31–40.
16. Doherty, D.G., et al. 1999. The human liver contains multiple populations of NK cells, T cells, and CD3+CD56+ natural T cells with distinct cytotoxic activities and Th1, Th2, and Th0 cytokine secretion patterns. *J. Immunol.* **163**:2314–2321.
17. Mazzaferro, V., et al. 1996. Liver transplantation for the treatment of small hepatocellular carcinomas in patients with cirrhosis. *N. Engl. J. Med.* **334**:693–699.
18. Mercer, D.F., et al. 2001. Hepatitis C virus replication in mice with chimeric human livers. *Nat. Med.* **7**:927–933.
19. Kneteman, N.M., et al. 2006. Anti-HCV therapies in chimeric scid-Alb/uPA mice parallel outcomes in human clinical application. *Hepatology.* **43**:1346–1353.
20. Tateno, C., et al. 2004. Near completely humanized liver in mice shows human-type metabolic responses to drugs. *Am. J. Pathol.* **165**:901–912.
21. Tseng, C.T., and Klimpel, G.R. 2002. Binding of the hepatitis C virus envelope protein E2 to CD81 inhibits natural killer cell functions. *J. Exp. Med.* **195**:43–49.
22. Crotta, S., et al. 2002. Inhibition of natural killer cells through engagement of CD81 by the major hepatitis C virus envelope protein. *J. Exp. Med.* **195**:35–41.
23. Wang, S.H., et al. 2008. Natural killer cells suppress full cycle HCV infection of human hepatocytes. *J. Viral Hepat.* **15**:855–864.
24. Kanto, T., and Hayashi, N. 2007. Innate immunity in hepatitis C virus infection: Interplay among dendritic cells, natural killer cells and natural killer T cells. *Hepatol. Res.* **37**(Suppl. 3):S319–S326.
25. Yamagiwa, S., et al. 2008. Sustained response to interferon-alpha plus ribavirin therapy for chronic hepatitis C is closely associated with increased dynamism of intrahepatic natural killer and natural killer T cells. *Hepatol. Res.* **38**:664–672.
26. Van Wauwe, J.P., De Mey, J.R., and Goossens, J.G. 1980. OKT3: a monoclonal anti-human T lymphocyte antibody with potent mitogenic properties. *J. Immunol.* **124**:2708–2713.
27. Chang, T.W., Kung, P.C., Gingras, S.P., and Goldstein, G. 1981. Does OKT3 monoclonal antibody react with an antigen-recognition structure on human T cells? *Proc. Natl. Acad. Sci. U. S. A.* **78**:1805–1808.
28. Chatenoud, L., et al. 1990. In vivo cell activation following OKT3 administration. Systemic cytokine release and modulation by corticosteroids. *Transplantation.* **49**:697–702.
29. Soza, A., et al. 2005. Pilot study of interferon gamma for chronic hepatitis C. *J. Hepatol.* **43**:67–71.
30. Jo, J., et al. 2009. Analysis of CD8+ T-cell-mediated inhibition of hepatitis C virus replication using a novel immunological model. *Gastroenterology.* **136**:1391–1401.
31. Penna, A., et al. 2007. Dysfunction and functional restoration of HCV-specific CD8 responses in chronic hepatitis C virus infection. *Hepatology.* **45**:588–601.
32. Ohdan, H., et al. 2003. Intraoperative near-infrared spectroscopy for evaluating hepatic venous outflow in living-donor right lobe liver. *Transplantation.* **76**:791–797.
33. Tanaka, Y., Ohdan, H., Onoe, T., and Asahara, T. 2004. Multiparameter flow cytometric approach for simultaneous evaluation of proliferation and cytokine-secreting activity in T cells responding to allo-stimulation. *Immunol. Invest.* **33**:309–324.
34. Guo, J.T., Bichko, V.V., and Seeger, C. 2001. Effect of alpha interferon on the hepatitis C virus replicon. *J. Virol.* **75**:8516–8523.
35. Tanabe, Y., et al. 2004. Synergistic inhibition of intracellular hepatitis C virus replication by combination of ribavirin and interferon- alpha. *J. Infect. Dis.* **189**:1129–1139.
36. Yokota, T., et al. 2003. Inhibition of intracellular hepatitis C virus replication by synthetic and vector-derived small interfering RNAs. *EMBO Rep.* **4**:602–608.
37. Tsuge, M., et al. 2005. Infection of human hepatocyte chimeric mouse with genetically engineered hepatitis B virus. *Hepatology.* **42**:1046–1054.
38. Hiraga, N., et al. 2007. Infection of human hepatocyte chimeric mouse with genetically engineered hepatitis C virus and its susceptibility to interferon. *FEBS Lett.* **581**:1983–1987.
39. Kimura, T., et al. 2008. Establishment of an infectious genotype 1b hepatitis C virus clone in human hepatocyte chimeric mice. *J. Gen. Virol.* **89**:2108–2113.

J Gastroenterol
DOI 10.1007/s00535-009-0162-3

ORIGINAL ARTICLE—LIVER, PANCREAS, AND BILIARY TRACT

Comparison of HCV-associated gene expression and cell signaling pathways in cells with or without HCV replicon and in replicon-cured cells

Yuki Nishimura-Sakurai · Naoya Sakamoto · Kaoru Mogushi · Satoshi Nagaie · Mina Nakagawa · Yasuhiro Itsui · Megumi Tasaka-Fujita · Yuko Onuki-Karakama · Goki Suda · Kako Mishima · Machi Yamamoto · Mayumi Ueyama · Yusuke Funaoka · Takako Watanabe · Seishin Azuma · Yuko Sekine-Osajima · Sei Kakinuma · Kiichiro Tsuchiya · Nobuyuki Enomoto · Hiroshi Tanaka · Mamoru Watanabe

Received: 2 September 2009 / Accepted: 2 November 2009

Abstract

Background Hepatitis C virus (HCV) replication is affected by several host factors. Here, we screened host genes and molecular pathways that are involved in HCV replication by comprehensive analyses using two genotypes of HCV replicon-expressing cells, their *cured* cells and naïve Huh7 cells.

Methods Huh7 cell lines that stably expressed HCV genotype 1b or 2a replicon were used. The *cured* cells were established by treating HCV replicon cells with interferon-alpha. Expression of 54,675 cellular genes was analyzed by GeneChip DNA microarray. The data were analyzed by using the KEGG Pathway database.

Results Hierarchical clustering analysis showed that the gene-expression profiles of each cell group constituted clear clusters of naïve, HCV replicon-expressed, and cured cell lines. The pathway process analysis between the replicon-expressing and the *cured* cell lines identified significantly altered pathways, including MAPK, steroid biosynthesis and TGF-beta signaling pathways, suggesting that these pathways were affected directly by HCV replication. Comparison of *cured* and naïve Huh7 cells identified pathways, including steroid biosynthesis and sphingolipid metabolism, suggesting that these pathways were required for efficient HCV replication. Cytoplasmic lipid droplets were obviously increased in replicon-expressing and *cured* cells as compared to naïve cells. HCV replication was significantly suppressed by peroxisome proliferator-activated receptor (PPAR)-alpha agonists but augmented by PPAR-gamma agonists.

Conclusion Comprehensive gene expression and pathway analyses show that lipid biosynthesis pathways are crucial to support proficient virus replication. These metabolic pathways could constitute novel antiviral targets against HCV.

Keywords DNA microarray · KEGG database · HCV replicon · Lipid metabolism

Abbreviations

HCV	Hepatitis C virus
TLR	Toll-like receptor
BMP	Bone morphogenetic protein

Y. Nishimura-Sakurai and N. Sakamoto contributed equally to this work.

Electronic supplementary material The online version of this article (doi:10.1007/s00535-009-0162-3) contains supplementary material, which is available to authorized users.

Y. Nishimura-Sakurai · N. Sakamoto (✉) · M. Nakagawa · Y. Itsui · M. Tasaka-Fujita · Y. Onuki-Karakama · G. Suda · K. Mishima · M. Yamamoto · M. Ueyama · Y. Funaoka · T. Watanabe · S. Azuma · Y. Sekine-Osajima · S. Kakinuma · K. Tsuchiya · M. Watanabe
Department of Gastroenterology and Hepatology,
Tokyo Medical and Dental University, 1-5-45 Yushima,
Bunkyo-ku, Tokyo 113-8519, Japan
e-mail: nsakamoto.gast@tmd.ac.jp

N. Sakamoto · M. Nakagawa · S. Kakinuma
Department for Hepatitis Control,
Tokyo Medical and Dental University, Tokyo, Japan

K. Mogushi · S. Nagaie · H. Tanaka
Information Center for Medical Science,
Tokyo Medical and Dental University, Tokyo, Japan

Y. Itsui
Department of Internal Medicine,
Soka Municipal Hospital, Saitama, Japan

N. Enomoto
First Department of Internal Medicine,
University of Yamanashi, Yamanashi, Japan

Published online: 12 December 2009

TGF	Transforming growth factor
FKBP	FK-binding protein
HSP	Heat shock proteins
FBS	Fetal bovine serum
YFP	Yellow fluorescence protein
FACS	Fluorescent activated cell sorting
RIN	RNA integrity number
SAM	Significance analysis of microarray
KEGG	Kyoto Encyclopedia of Genes and Genomes
EGID	NCBI Entrez Gene ID
RT-PCR	Reverse transcription-polymerase chain reaction
MTS	Dimethylthiazol carboxymethoxyphenyl sulfophenyl tetrazolium
PPAR	Peroxisome proliferator-activated receptor

Introduction

Hepatitis C virus (HCV) infection is one of the most important causative agents of acute and chronic hepatitis, liver cirrhosis and hepatocellular malignancies [1]. Currently, the most efficient combination treatment of ribavirin plus peginterferon can eliminate the virus in almost half of the patients treated [2, 3]. Thus, it is our high priority goal to understand the HCV life cycle precisely, to identify cellular cofactors for HCV replication and to develop new class antiviral therapeutics.

Molecular analyses of the HCV life cycle, virus–host interactions, and mechanisms of liver cell damage by the virus are not understood completely, mainly because of the lack of cell culture systems. These problems have been partly overcome by the development of the HCV subgenomic replicon [4] and HCV cell culture systems [5, 6]. These systems have allowed us to study the complete HCV life cycle: virus-cell entry, translation, protein processing, RNA replication, virion assembly and virus release.

Several host proteins and drugs have been reported to have a direct affect on HCV replication in vitro [7]. These include factors that affect immune responses (interferons and their related genes [8, 9], RIG-I, TLRs [10]), cell proliferation (BMP7 [11], TGF-beta [12], nucleolin [13]), molecular chaperone function (cyclophilin [14], ER-stress proteins [15], FKBP [16], HSP27 [17], HSP90 [18]) and lipid metabolism (cholesterol, sphingolipid [19]). However, it is often difficult to determine whether these genes are changed by HCV replication or the changes are essential for HCV replication in the host cells.

In this study, we investigated the effects of host cellular gene expression using our HCV replicon system [20, 21]. We performed DNA microarray analyses using cells expressing the replicons, the corresponding *cured* cells, from which the replicon had been eliminated by prolonged treatment with interferon-alpha, and naïve Huh7 cells. Furthermore, we investigated the signaling pathways using DNA microarrays to study molecular pathways that are involved in the HCV life cycle and its pathogenesis.

Materials and methods

Cells and cell culture

Huh7 cells were maintained in Dulbecco's modified minimal essential medium (Sigma, St. Louis, MO) supplemented with 10% fetal calf serum at 37°C under 5% CO_2. To maintain cell lines carrying the HCV replicon (Huh7/Rep cells), G418 (Nakalai Tesque, Kyoto, Japan) was added to the culture medium to a final concentration of 500 μg/ml.

HCV replicon and cell culture

The HCV-1b replicon plasmid, pHCV1bneo-delS, was provided by Dr. Christoph Seeger (Fox Chase Cancer Center, Philadelphia, PA) [22]. HCV-2a replicon plasmid, pSGR-JFH1, was provided by Dr. Takaji Wakita (National Institute of Infectious Diseases, Tokyo, Japan). The neomycin phosphotransferase (Neo) gene of pHCV1bneo-delS and pSGR-JFH1 was replaced by a chimeric gene coding for yellow fluorescent protein fused in-frame with the foot-and-mouth disease virus peptide 2A (P2A) autocleavage motif followed by neomycin phosphotransferase, which we designated *Yeo* (Fig. 1) [23]. An HCV *Feo*-replicon that expresses chimeric firefly luciferase and the neomycin resistance gene has been described [20, 21]. In vitro replicon RNA synthesis, RNA transfection and selection of G418-resistant cell lines were carried out as described previously [21, 24]. Briefly, replicon RNAs were transfected into Huh7 cells. By cell culture in the presence of G418, we established Huh7 cell lines that stably express the *Yeo*-replicons: Huh7/Rep-1b-*Yeo* and Huh7/Rep-2a-*Yeo*.

Fluorescence microscopy and FACS analysis

The cells were plated onto eight-well chamber slides (Lab-Tek® Chamber Slide™ System, Nalgen Nunc International, Rochester, NY), and the YFP expression was detected by fluorescence microscopy (BZ-8000,

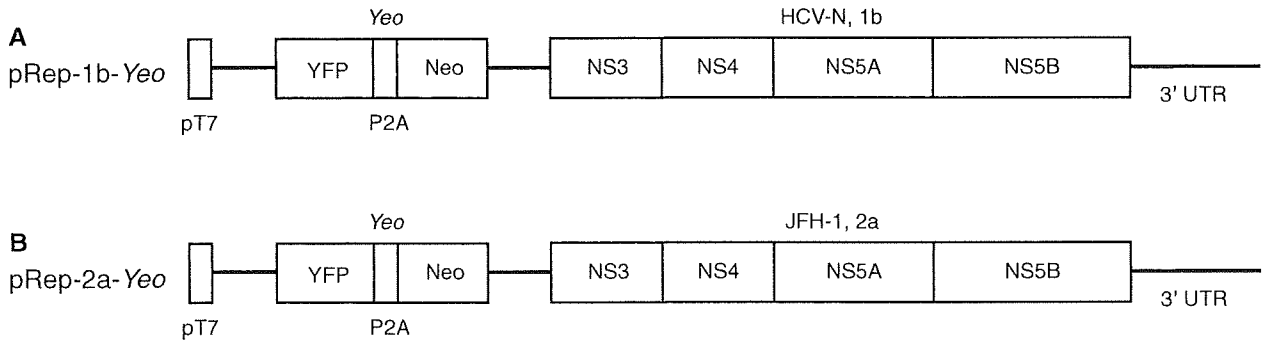

Fig. 1 Structure of replicon plasmid constructs. A hepatitis C virus (HCV) replicon plasmid, pRep-1b-Yeo (**a**) and pRep-2a-Yeo (**b**), was reconstructed from pHCV1bneo-delS [22] and pSGR-JFH1 [47] by replacing the neomycin phosphotransferase (Neo) gene with a fusion gene of yellow fluorecence protein (YFP) and Neo, which we designate "*Yeo*." *NS* Nonstructural region, *pT7* T7 promoter, *3'UTR* 3'untranslated region, *P2A* foot-and-mouth disease peptide 2A (see also "Materials and methods") [23]

KEYENCE, Osaka, Japan) and FACS Caliber using CellQuest software (BD Biosciences, Flanklin Lakes, NJ).

Cell sorting

Cells were treated for 5 min with trypsin/EDTA at 37°C and then resuspended in 10% FBS/DMEM. A single cell suspension was prepared by passage through a 35-μm nylon filter. The cell populations that support a high level of *Yeo*-replicon expression (Huh7/Rep-1b-*Yeo*^{high} and Huh7/Rep-2a-*Yeo*^{high}) were separated using a FACS Vantage SE cell-sorting system (BD Biosciences). The YFP-directed fluorescence of sorted cells was confirmed by fluorescence microscopy and FACS.

Establishment of the cured Huh7 cells

Cured Huh7 cells (cHuh7) were established by eliminating the HCV replicon from the *Yeo*-1b^{high} and -2a^{high} replicon expressing Huh7 cells by treatment with 100 U/ml of interferon-alpha for 14 days [6, 25]. Clearance of replicon RNA was confirmed by FACS analysis and by the loss of resistance to G418.

RNA preparation and microarray hybridization

Total cellular RNA was extracted from the 1b^{high} and 2a^{high} *Yeo*-replicon cells, *cured*-1b and -2a cells and naïve Huh7 cells using ISOGEN (Wako). Integrity of obtained RNA was assessed using Agilent 2100 Bioanalyzer (Agilent Technologies, Palo Alto, CA). All samples had an RNA Integrity Number (RIN) greater than 9.4 [26]. Complementary RNA was prepared from 1 μg total RNA, using one-cycle target labeling and a control reagents kit (Affymetrix, Santa Clara, CA). Hybridization and signal detection of the Human Genome U133 Plus 2.0 array (Affymetrix) were performed in accordance with the manufacturer's instructions. Assays were performed in duplicate.

Analysis of gene expression data

A total of ten microarray datasets was normalized using the robust multi-array average (RMA) method under R 2.8.1 statistical software (http://www.R-project.org). Estimated gene expression levels were log_2-transformed, data from 62 control probe sets were removed, and we selected 18,613 probe sets that were categorized as "present" or "marginal" among all samples. We performed two sets of gene comparisons to examine effects of HCV replicons on host cellular gene expression: one was the *high Yeo*-replicon-expressing cells versus *cured* cells and the other was parental Huh7 cells versus *cured* cells. We selected differently expressed genes using the significance analysis of microarray (SAM) as described by Tusher et al. [27], and the fold changes and the Q-values were calculated for each probe sets. We used delta = 0.1 as a cutoff parameter for SAM. A hierarchical clustering with selected genes was performed with R software. Euclidean distance was used to calculate the similarity matrix among genes or cell conditions, respectively. The complete linkage method was used for agglomeration.

Molecular pathway analysis and visualization of gene expression data

We used the KEGG Pathway database to investigate the molecular reactions and pathways that showed significant gene expression changes [28]. The KEGG Pathway is a database of biological systems, consisting of over 4,252 genes and 204 molecular pathway-wiring diagrams of interaction and reaction networks (http://www.genome.jp/kegg/pathway.html). Prior to the pathway analysis, we selected probe sets that were differentially expressed

between Huh7 and *cured* cells and between *cured* cells and replicon cells. For Huh7 versus *cured* cells analyses, we selected probe sets that showed 20% upregulation or downregulation (i.e., fold change of grater than 1.2) in both Huh7 versus *cured*-1b and Huh7 versus *cured*-2a cells. For replicon cell versus *cured* cell analyses, we selected probe sets that showed 20% upregulation or downregulation in both *cured*-1b versus replicon-1b cells or *cured*-2a versus replicon-2a cells. Association between the obtained gene list and each pathway was evaluated by Fisher's exact test. The significance level for KEGG analysis was set to a false discovery rate (FDR) of lower than 0.3 using the Benjamini and Hochberg method [29].

We next visualized functional associations between the differentially expressed genes and biological pathway processes. The KEGG Pathway provides a reference knowledge base for linking genomes to biological systems and also to environments by the processes of Pathway mapping and BRITE mapping. NCBI Entrez Gene IDs (EGIDs) for each gene in the pathways were extracted from the database. The relationship between probe sets on the microarray and EGIDs was obtained from a gene annotation file provided by Affymetrix. Thereafter, gene expression changes were mapped on the pathway by combining the results of fold-change analyses with the data sets above.

Real-time PCR analysis of mRNA expression

To confirm the results of the microarray analysis, we examined the expression levels of several mRNA by real-time RT-PCR (7500 Real Time PCR Systems, Applied Biosystems, Foster City, CA). Single-stranded cDNA was synthesized from total RNA using SuperScript II reverse transcriptase (Invitrogen) and random hexamers (Takara Bio Inc., Shiga, Japan) as primers. Expression of mRNA was quantified using QuantiTect SYBR Green PCR master Mix (QIAGEN, Valencia, CA). The primers used were as follows: HMGCR, SQLE, CYP51A1, TM7SF2, NSDHL, EBP and beta-actin. The nucleotide sequences of primers and corresponding product sizes are as indicated (see Supplementary Table 1).

Oil red O staining

Huh7 cells, replicon cells and *cured* cells were cultured on 18-mm-round micro cover glasses (Matsunami, Tokyo, Japan). These cells were fixed with 4% paraformaldehyde for 5 min at room temperature. After washing with PBS, the cells were permeabilized with 0.05% Triton X-100 in PBS for 5 min at room temperature. Staining of intracellular neutral lipids was performed with Oil red O, and nuclei were stained with Mayer's hematoxylin using Oil red O stain kit procedure (Diagnostic Biosystems Inc., Pleasanton, CA).

Immunofluorescence analysis

Huh7 cells, replicon cells and *cured* cells were cultured on 18-mm-round micro cover glasses. For immunostaining, the cells were fixed in 4% paraformaldehyde for 5 min at room temperature. For detection of HCV-NS5A, cells were incubated with the primary antibody (Biodesign International, Saco, ME) for 1 h at 37°C. The fluorescent secondary antibodies were Alexa Fluor 594 goat anti-mouse IgG antibody (Invitrogen, Carlsbad, CA). Nuclei were labeled with 4′,6-diamidino-2-phenylindole (DAPI). Lipid droplets were visualized with BODIPY 493/503 (Invitrogen). Analysis was performed on a Delta-Vision microscope system (Applied Precision, Seattle, WA).

Luciferase-based expression analysis of HCV replicon and analysis of cell viability

Huh7/Rep-Feo cells [20, 21] were cultured with various concentrations of peroxisome proliferator-activated receptor (PPAR)-alpha and -gamma agonists. After 48 h of culture, levels of HCV replication were quantified by internal luciferase assay using a Bright-Glo Luciferase Assay System (Promega). Assays were performed in triplicate, and the results were expressed as mean ± SD as percentages of the controls. To evaluate cell viability, dimethylthiazol carboxymethoxyphenyl sulfophenyl tetrazolium (MTS) assay was performed using a Cell Titer 96 Aqueous One Solution Cell Proliferation Assay (Promega) according to manufacturer's directions.

Statistical analyses

Statistical analyses were performed using the Student's *t*-test, and *P*-values of less than 0.05 were considered as statistically significant.

Results

Fluorescence detection of Yeo replicon

Genotypes 1b and 2a *Yeo*-replicon RNAs were stably transfected into Huh7 cells (Huh7/Rep-1b-Yeo and Huh7/Rep-2a-Yeo, respectively, Fig. 1). In these transfected cells, expression of the HCV replicon was visualized by HCV-IRES-driven, YFP-mediated fluorescence (Fig. 2, left panels). The expression levels of individual cells could be measured by fluorescence intensity and cytogram analysis using flow cytometry (Fig. 2, right panels).

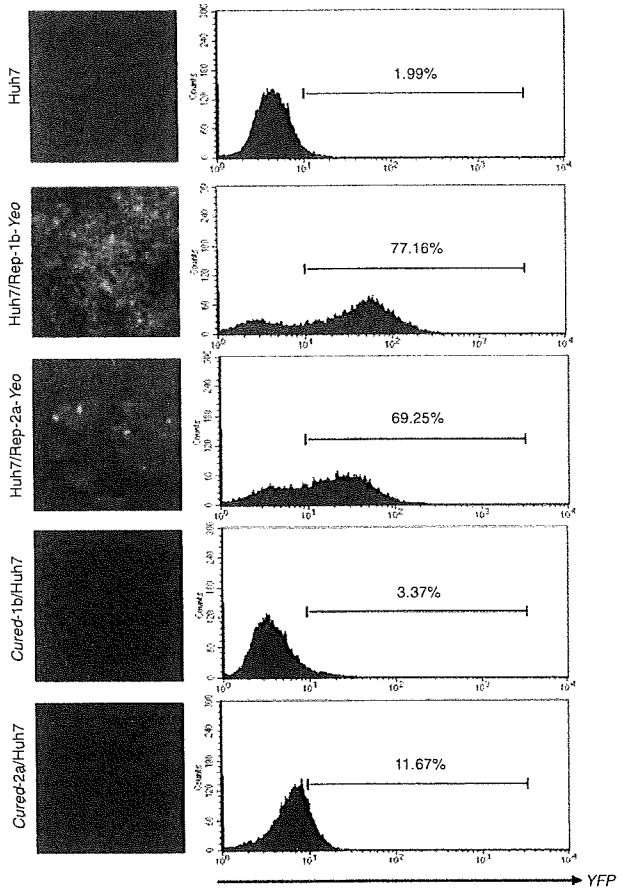

Fig. 2 Visualization of YFP replicon expression. Detection of YFP expression by fluorescence microscopy analysis and of intracellular YFP expression by FACS analysis

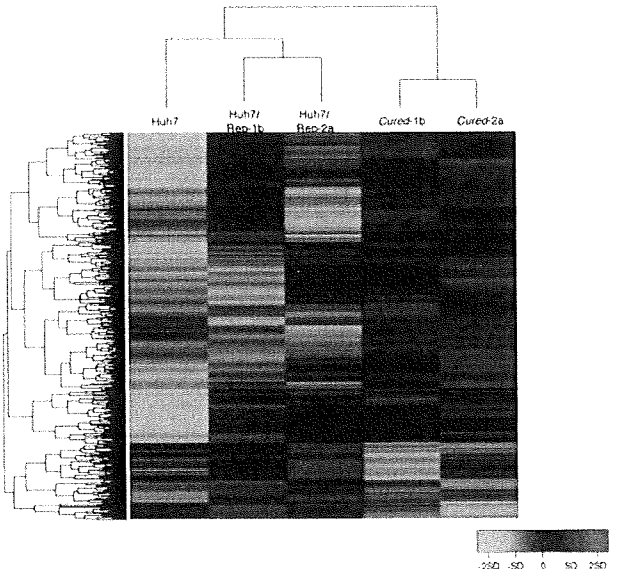

Fig. 3 Hierarchical clustering of gene expression profiles obtained from the 1b and 2a Yeo-replicon expressiong cells, cured cells and Huh7. The 1,870 probe sets that changed expression more than 1.2-fold in either Huh7 versus *cured* or *cured* versus replicon were selected. Dendrograms show the classification determined by hierarchical clustering analysis. *Red* and *green colors* indicate relative overexpression and underexpression, respectively

Our initial trial was to compare gene expression profiles between replicon-expressing cells and parental Huh7 cells. However, these comparisons identified gene expressional changes induced by HCV infection and by adaptation of the host cell to support efficient HCV replication, because transfection of replicon RNA and G418-treatment of cells resulted in selection of a cell population that can support a high level of HCV subgenomic replication. Therefore, we used *cured* cell lines, which were established from Huh7/Rep-1b-Yeo and -2a-Yeo by interferon-alpha treatment. These cured cell lines are highly permissive for HCV replication on re-introduction of virus or replicon RNA (Fig. 2). With these backgrounds, we performed two sets of gene comparison using microarray analyses: comparison of replicon-expressing cell lines (Huh7/Rep-1b-Yeo and Huh7/Rep-2a-Yeo) and *cured* cells (Cured-1b/Huh7 and Cured-2a/Huh7) was intended to identify genes that are affected by HCV replication, and comparison of parental Huh7 cells and *cured* cell lines was intended to identify genes that are essential for a high level of HCV replication in cultured cells.

Hierarchical clustering gene expression profiles in naïve, replicon-expressing and cured cells

Datasets from the microarrays were normalized using the robust multi-array average (RMA) method, and differentially expressed genes were extracted in replicon cells, *cured* cells and naïve Huh7 cells. Gene expression profiles were well correlated each other between duplicate microarray data from the same cell line with the Pearson's correlation coefficients (R^2) of greater than 0.975 (see Supplementary Fig. 1). In this analysis, 1,870 probe sets showed differences in expression levels of more than 1.2-fold under delta <0.1 in either Huh7 versus *cured* (1,516 probe sets) or *cured* versus replicon (372 probe sets). A hierarchical clustering analysis showed that the gene-expression profiles of each cell group constituted clear clusters, Huh7/Rep-2a and Huh7/Rep-1b, Cured-2a and Cured-1b, and Huh7 cells (Fig. 3). Among genes whose expression differed significantly between replicon-expression cells and *cured* cells, 15 showed changes of more than two-fold (Table 1). These included cell cycle- or cell growth-related genes (nuclear protein 1, growth duf-ferentiation factor 15, urothelial cancer associated 1, inhibin and tubulin), oncogene (Ras-related GTP binding D) and interferon-related gene (IFIM3). On the other hand, 37

Table 1 Microarray analysis: genes for which the expression changed more than two-fold in Rep-1b/Huh7 and Rep-2a/Huh7 cells compared to their *cured* cells

Probe set	Title	Rep1b/cured1b		Rep2a/cured2a	
		Fold change	*Q*-value	Fold change	*Q*-value
209230_s_at	Nuclear protein 1	5.41	0.00	13.78	7.44
221523_s_at	Ras-related GTP binding D	3.82	0.00	2.32	24.60
221524_s_at	Ras-related GTP binding D	3.17	0.00	2.40	17.08
205923_at	Reelin	3.14	0.00	2.70	12.42
200924_s_at	Hypothetical protein LOC442497/solute carrier family 3 (activators of dibasic and neutral amino acid transport), member 2	2.84	0.00	2.63	0.69
221577_x_at	Growth differentiation factor 15	2.62	0.00	3.16	0.00
233030_at	Patatin-like phospholipase domain containing 3	2.07	0.00	2.31	3.16
201471_s_at	Sequestosome 1	2.52	0.81	2.10	2.45
227919_at	Urothelial cancer associated 1	5.09	0.90	2.90	54.18
207076_s_at	Argininosuccinate synthetase 1	2.99	0.90	2.22	61.28
205749_at	Cytochrome P450, family 1, subfamily A, polypeptide 1	2.69	0.90	2.63	4.55
217127_at	Cystathionase (cystathionine gamma-lyase)	2.32	3.05	2.38	6.54
210587_at	Inhibin, beta E	2.51	4.25	3.89	2.45
214023_x_at	Tubulin, beta 2B	2.41	4.25	4.31	54.18
212203_x_at	Interferon induced transmembrane protein 3 (1-8U)	2.34	5.75	2.09	54.18

genes were up-regulated by more than two-fold between *cured* and naïve cells (Table 2), which included genes such as chemokine (CCL14), solute carrier family and metallothionein family.

Pathway process analyses and hierarchical clustering of genes in each functional category

Using the KEGG Pathway database, we analyzed pathway processes that were altered between replicon-expressing cells and *cured* cells as well as between *cured* cells and Huh7 cells (Supplementary Tables 2, 3). Comparison of the pathway processes between replicon-expressing and *cured* cells identified six pathways that showed differences of FDR < 0.3, including pathways related to MAPK ($P = 4.0 \times 10^{-4}$, FDR 0.08), biosynthesis of steroids ($P = 4.21 \times 10^{-3}$, FDR 0.21) and TGF-beta ($P = 8.4 \times 10^{-3}$, FDR 0.29) (KEGG Pathway maps for each significant pathways are shown in Supplementary Fig. 2A–F). Comparison of the pathway processes between *cured* and naïve Huh7 cells identified 11 significant pathways (KEGG Pathway maps for each significant pathway are shown in Fig. 5 and Supplementary Fig. 3A–J). These included pathways that were related to TGF-bata ($P = 8.42 \times 10^{-3}$), cell cycle ($P = 9.0 \times 10^{-3}$) and sphingolipid metabolism ($P = 1.32 \times 10^{-2}$). Interestingly, there were significant changes in the biosynthesis of steroids ($P = 1.75 \times 10^{-4}$) between cured and naïve Huh7 cells. These results suggested that several lipid metabolism processes were substantially associated with efficient HCV replication in host cells.

Hierarchical clustering analyses of representative genes included in functional pathway categories

Based on pathway process analyses using the KEGG database, we performed hierarchical clustering analyses of each functional subset of genes (fold change >1.2, Fig. 4a–c). The cell cycle, cholesterol biosynthesis and sphingolipid metabolism-related genes demonstrated clear clusters in replicon cells, *cured* cell and parental Huh7, respectively. In particular, cholesterol biosynthesis-related genes were activated in replicon cells and *cured* cells.

Mapping between pathway information and gene expression data

Knowing that cholesterol metabolism pathway was changed substantially in *cured* cells, we performed graphical mapping of the related genes to the KEGG Pathway map database (Fig. 5). Similar to the pathway analyses, cholesterol biosynthesis related genes, which are involved in the mevalonate pathway or sterol biosynthesis, were clearly activated in *cured* cells compared to naïve Huh7 (Fig. 5).

To verify the microarray results, we performed real-time RT-PCR of cholesterol biosynthesis-related genes including HMGCR, SQLE, NSDHL, CYP51A1, TM7SF2 and EBP. All the genes were upregulated in replicon-expressing and *cured* cells compared to the naïve Huh7 cells (Fig. 6). These results were consistent with the microarray data.

Table 2 Microarray analysis: genes for which the expression changed more than two-fold in *cured*-1b and *cured*-2a cells compared to Huh7

Probe set	Title	Cured1b/Huh7		Cured2a/Huh7	
		Fold change	*Q*-value	Fold change	*Q*-value
210390_s_at	Chemokine (C–C motif) ligand 14/15	4.49	0.00	2.56	0.00
221168_at	PR domain containing 13	2.38	0.00	2.15	0.00
1553995_a_at	5′-nucleotidase, ecto (CD73)	2.15	0.00	3.64	0.36
204897_at	Prostaglandin E receptor 4 (subtype EP4)	2.07	2.40	2.19	0.36
214522_x_at	Histone cluster 1, H2ad/H3d	3.01	4.12	2.98	0.46
214472_at	Histone cluster 1, H2ad/H3a-j	3.36	5.08	3.53	0.46
218280_x_at	Histone cluster 2, H2aa3/H2aa4	4.65	5.20	5.17	0.61
232035_at	Histone cluster 1, H4a-f, H4 h-l/histone cluster 2, H4a-b/histone cluster 4, H4	5.56	6.51	5.37	0.95
214455_at	Histone cluster 1, H2bc, H2be, H2bf, H2bg, H2bi	4.72	6.51	2.68	0.61
202708_s_at	Histone cluster 2, H2be	4.48	6.51	5.31	0.95
214290_s_at	Histone cluster 2, H2aa3/H2aa4	4.06	6.51	2.98	2.08
209398_at	Histone cluster 1, H1c	3.40	6.51	3.60	2.08
230795_at	–	2.91	6.51	4.51	0.95
1553994_at	5′-nucleotidase, ecto (CD73)	2.29	6.51	2.31	3.34
208180_s_at	Histone cluster 1, H4a-f, H4 h-l/histone cluster 2, H4a, H4b/histone cluster 4, H4	6.27	7.65	3.40	1.46
215779_s_at	Histone cluster 1, H2bc, H2be, H2bf, H2bg, H2bi	3.53	7.65	5.86	1.46
206110_at	–	3.82	9.12	10.68	0.00
206535_at	Solute carrier family 2 (facilitated glucose transporter), member 2	3.58	9.12	2.84	5.02
213880_at	Leucine-rich repeat-containing G protein-coupled receptor 5	2.81	9.12	3.02	5.02
210387_at	Histone cluster 1, H2bc, H2be, H2bf, H2bg, H2bi	3.24	10.68	2.28	11.66
203044_at	Chondroitin sulfate synthase 1	2.36	11.85	2.67	2.08
207102_at	Aldo-keto reductase family 1, member D1 (delta 4-3-ketosteroid-5-beta-reductase)	2.14	13.35	5.58	0.36
219596_at	THAP domain containing 10	2.20	16.73	3.32	2.08
217997_at	Pleckstrin homology-like domain, family A, member 1	2.15	23.48	3.01	3.34
217996_at	Pleckstrin homology-like domain, family A, member 1	2.12	23.48	2.21	11.66
217165_x_at	Metallothionein 1F	3.36	29.61	3.25	11.66
213629_x_at	Metallothionein 1F	3.13	29.61	3.70	11.66
210524_x_at	–	2.39	29.61	2.46	17.81
206143_at	Solute carrier family 26, member 3	2.35	29.61	2.49	17.81
212859_x_at	Metallothionein 1E	3.46	35.93	4.07	11.66
208581_x_at	Metallothionein 1X	3.31	35.93	3.52	17.81
204326_x_at	Metallothionein 1X	3.24	35.93	3.49	17.81
211456_x_at	Metallothionein 1 pseudogene 2	3.19	35.93	3.71	17.81
206461_x_at	Metallothionein 1H	3.09	35.93	3.49	17.81
216336_x_at	Metallothionein 1E, 1H, 1 M/metallothionein 1 pseudogene 2	3.02	35.93	3.27	17.81
212185_x_at	Metallothionein 2A	2.92	35.93	2.85	17.81
204745_x_at	Metallothionein 1G	2.73	35.93	3.31	17.81

Detection of intracellular lipid droplets in naïve, replicon-expressing and cured cells

Because several lipid-related pathways were extracted (Supplementary Tables 2 and 3), we examined phenotypes of the cell lines featuring different lipid metabolism gene expression profiles by carrying out detection of cellular lipid droplets (Fig. 8a, b). The cells were stained by Oil red O or BODIPY493/503, dye solutions specific for neutral lipids. We found a large number of lipid droplets in the cytoplasm of each Huh7 cell line. The number of lipid droplets obviously was increased more in

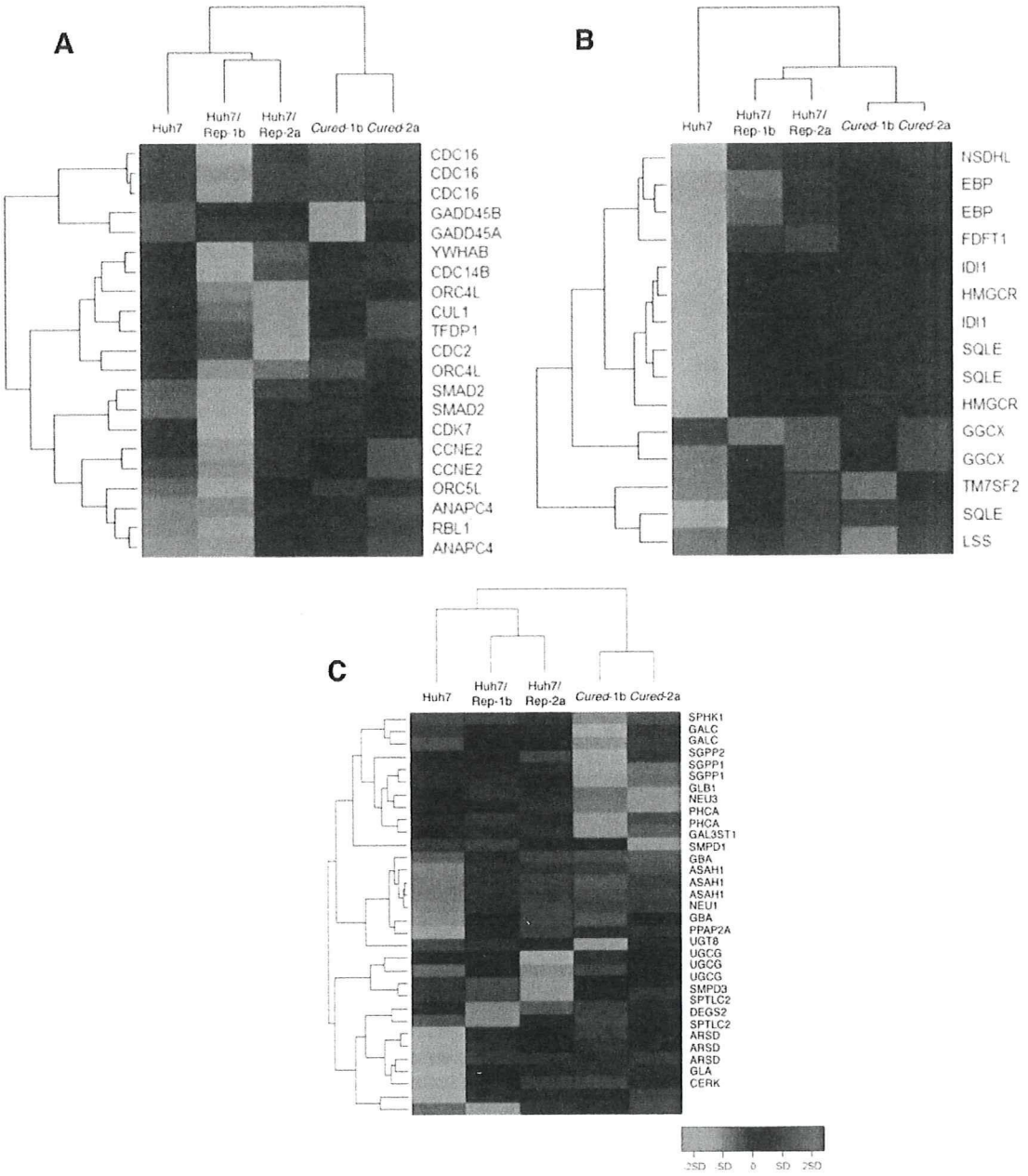

Fig. 4 Hierarchical clustering of representative genes included in each KEGG Pathway map. **a** Cell cycle, **b** cholesterol biosynthesis, **c** sphingolipid metabolism. Dendrograms shows the classification determined by hierarchical clustering analysis. *Red* and *green colors* indicate relative overexpression and underexpression, respectively

the two replicon-expressing cells and the *cured* cells than in the parental Huh7 cells. Lipid and HCV-NS5A double staining showed an increase in lipid droplets in cells that expressed HCV proteins (Fig. 8b). Analyses of the KEGG fatty acid metabolism pathway showed that a substantial number of the genes of these pathways were up-regulated in the *cured* cells compared to the naïve cells, although these could not reach statistical significance (Fig. 7).

Effects of hepatitis C virus replication by PPAR-alpha and gamma agonists

To assess the effects of lipid metabolic status on the intracellular replication of the HCV genome, Huh7/Rep-Feo cells were cultured with various concentrations of several PPAR-alpha agonists (clofibrate, fenofibrate and bezafibrate) and gamma agonists (pioglitazone and troglitazone) (Fig. 9). The luciferase activities of the Huh7/